Chem. Senses 33: 803–813, 2008

doi:10.1093/chemse/bjn043
Advance Access publication July 16, 2008

Pharmacological Investigation of Protein Kinase C- and cGMP-Dependent Ion Channels in Cultured Olfactory Receptor Neurons of the Hawkmoth *Manduca sexta*

Jan Dolzer[1], Steffi Krannich[1,2] and Monika Stengl[1,2]

[1]Department of Biology, Animal Physiology, Philipps-University of Marburg, Karl-von-Frisch-Strasse 8, Marburg D-35032, Germany and [2]Institute of Biology, Animal Physiology, University of Kassel, Heinrich-Plett-Strasse 40, Kassel D-34132, Germany

Correspondence to be sent to: Monika Stengl, Department of Biology, Animal Physiology, Philipps-University of Marburg, Karl-von-Frisch-Strasse 8, Marburg D-35032, Germany. e-mail: stengl@staff.uni-marburg.de

Abstract

In the hawkmoth *Manduca sexta*, pheromone stimuli of different strength and duration rise the intracellular Ca^{2+} concentration in olfactory receptor neurons (ORNs). While second-long pheromone stimuli activate protein kinase C (PKC), which apparently underlies processes of short-term adaptation, minute-long pheromone stimuli elevate cyclic guanosine monophosphate (cGMP) concentrations, which correlates with time courses of long-term adaptation. To identify ion channels involved in the sliding adjustment of olfactory sensitivity, inside-out patch clamp recordings on cultured ORNs of *M. sexta* were performed to characterize Ca^{2+}-, PKC-, and cGMP-dependent ion channels. Stepping to positive holding potentials in high intracellular Ca^{2+} elicits different Ca^{2+}-dependent ion channels, namely small-conductance channels (2–20 ps), medium-conductance channels (20–100 ps), and large-conductance channels (>100 ps). Ion channels of 40, 60, and 70 ps opened after PKC activation, whereas 10- and >100-ps channels were observed less frequently. Application of 8-bromo cyclic guanosine monophosphate opened 55- and 70-ps channels and increased the open probability of >100-ps channels, whereas even in the presence of phorbol ester 40-ps channels were inhibited. Thus, cGMP elevations activate a different set of ion channels as compared with PKC and suppress at least one PKC-dependent ion channel.

Key words: insect olfactory transduction, ion channels, *Manduca sexta*, olfactory adaptation, patch clamp

Introduction

Adaptation, the adjustment of sensitivity in response to adequate stimulation, enlarges the dynamic range of an olfactory receptor neuron (ORN) without loss of resolution and provides the first stage of processing sensory information. In vertebrate ORNs, 3 different mechanisms of olfactory adaptation coexist: short-term adaptation, desensitization, and long-term adaptation. These 3 olfactory adaptation mechanisms vary in their time courses and pharmacological properties (Zufall and Leinders-Zufall 2000). The influx of Ca^{2+} through cyclic nucleotide–gated (CNG) channels and the Ca^{2+}-dependent modulation of CNG channels plays a crucial role as a feedback signal in vertebrate olfactory adaptation (Zufall and Leinders-Zufall 2000; Matthews and Reisert 2003; Pifferi et al. 2006). In insects, most studies on olfactory adaptation mechanisms were accumulated in moths (Zack-Strausfeld and Kaissling 1986; Kaissling et al. 1986; Marion-Poll and Tobin 1992; Dolzer et al. 2003; Flecke et al. 2006). In *Manduca sexta*, our extracellular recordings revealed at least 3 different mechanisms of olfactory adaptation. One that decreases the amplitude and the initial slope of the sensillum potential, one that accelerates the repolarization phase, and one that decreases the action potential response even further than the parameters of the sensillum potential (Dolzer et al. 2003). Whether these different moth olfactory adaptation mechanisms correspond to the different mechanisms in vertebrates and what types of ion channels are involved in moths remained elusive.

Previous patch clamp studies in moth ORNs showed that pheromone stimulation activates a phospholipase C which elicits transient IP_3-dependent Ca^{2+} influx (Boekhoff et al. 1990; Stengl 1994; Wegener et al. 1997; Stengl et al. 1999). The transient influx of Ca^{2+} triggers a temporal sequence of Ca^{2+}-dependent currents (Stengl 1993). Within the first milliseconds of pheromone application, a directly

Ca^{2+}-dependent, Ca^{2+}-permeable inwardly rectified cation channel opened with a conductance of about 20 ps at 25 mV and 50 ps at –100 mV holding potential (Stengl et al. 1992; Stengl 1993). Because the lipophilic pheromone cannot be easily removed except after addition of pheromone-binding protein or bovine serum albumine, pheromone was usually present for several seconds and minutes after application (Stengl et al. 1992; Stengl 1993). This led to further elevation of the intracellular Ca^{2+} concentration as measured via patch clamp recordings (or via Ca^{2+} imaging with FURA, Stengl M, Lindemann B, unpublished). The intracellular Ca^{2+} increase finally blocked Ca^{2+}-dependent cation channels and caused activation of a protein kinase C (PKC). PKC activated tetraethylammonium (TEA)-blockable cation currents with apparently little Ca^{2+} conductance, caused further depolarization, but decreased the intracellular Ca^{2+} concentrations (Stengl 1993, 1994; Stengl et al. 1999). We, therefore, hypothesize that the duration of the pheromone stimulus, the corresponding increase of the intracellular Ca^{2+} concentration, and the resulting regulation of PKC activity determine pheromone sensitivity of the antenna and might underlie mechanisms of short-term adaptation. Short-term adaptation in moths implies a fast decrease in pheromone sensitivity and lasts less than 5 min, whereas long-term adaptation occurs more slowly and can last for several hours. Corresponding with time courses of long-term adaptation, pheromone stimuli induced minute-long rises in cyclic guanosine monophosphate (cGMP) levels in moth antennae (Ziegelberger et al. 1990; Boekhoff et al. 1993; Redkozubov 2000). In *M. sexta*, minute-long pheromone stimulation resulted in cGMP rises in pheromone-sensitive ORNs and their respective supporting cells (Stengl et al. 2001) and adapts the action potential response but not the sensilla potential (Flecke et al. 2006). This suggests that Ca^{2+}-, PKC-, and cGMP-dependent processes might underlie mechanisms of olfactory short- and long-term adaptation in *M. sexta* and might orchestrate a sliding adjustment of odor sensitivity.

To further test this hypothesis, we initially characterized Ca^{2+}-, PKC-, and cGMP-dependent ion channels in cultured ORNs of *M. sexta*. Inside-out patches were excised into bath solutions with high (intracellular) Ca^{2+} to activate Ca^{2+}-dependent cation channels, previously shown to be pheromone dependent (Stengl 1993, 1994). Then, the Ca^{2+}-dependent ion channels were stimulated with the PKC activator phorbol ester (phorbol 12-myristate 13-acetate [PMA]) and/or the membrane-permeable cGMP analog 8-bromo cyclic guanosine monophosphate (8bcGMP) to search for differential second messenger modulation. Application of PKC and cGMP activated different populations of cation channels. Furthermore, cGMP blocked at least one population of cation channels that opened PKC dependently. Thus, our results are consistent with our hypothesis that different sets of second messenger–mediated ion channels are involved in the different mechanisms of olfactory adaptation, which depend on stimulus length and strength.

Materials and methods

Unless indicated otherwise, all chemicals and biochemicals were obtained from Sigma (Deisenhofen, Germany) and all cell culture media from Gibco (Karlsruhe, Germany). The salts for the electrophysiological salines were obtained from Merck (Frankfurt/M, Germany).

Cell cultures

Cell cultures were prepared according to Stengl and Hildebrand (1990). Briefly, male pupae were staged using external markers (Jindra et al. 1997). For dispersion, animals were anesthetized by cooling, and the antennae were dissected in Hank's balanced salt solution with penicillin/streptomycin (HBSS/PS). Antennal tubes were washed in HBSS/PS and incubated in HBSS/PS + 7 mM ethyleneglycol-bis(aminoethylether)-tetraacetic acid (EGTA) at 37 °C for 5 min. The tissue was digested with papain (1 mg/ml in HBSS/PS) in 2 batches for 5 and 10 min at 37 °C, respectively. The digestion was stopped by adding Leibovitz medium (L-15) supplemented with 10% fetal bovine serum. Cells were centrifuged at 70–110 relative centrifugal force for 5–8 min, and the pellet was resuspended in HBSS/PS. The cells were plated out in glass bottom culture dishes, which were coated with concanavalin A and poly-L-lysin, and allowed to settle for 15–30 min before adding 1 ml of a 2:1 cell culture medium. The medium was replaced completely within 24 h after dispersion. Every 4–7 days, part of the medium was replaced subsequently. The cell cultures were used for electrophysiology from 10 days up to 4 weeks after plating.

Solutions

All solutions were adjusted to pH 7.1–7.2. The osmolality was adjusted with mannitol to 370–390 mosmol for bath solutions and 330–350 mosmol for pipette solutions, respectively. During recordings, cells were kept in 1-ml bath solution. Drugs were applied either by puff application with a PicoSpritzer (General Valve, Fairfield, NJ) or pipetted into the bath. Each recording was started under standard bath and high CsCl intracellular pipette conditions to activate sustained Ca^{2+}-dependent nonselective cation channels and to minimize K^+ channel activity. To recognize and stabilize Ca^{2+}-dependent inwardly rectified cation channels, the Ca^{2+} concentration in the patch pipette was buffered. Then, to further characterize Ca^{2+}-dependent ion channels, voltage step protocols were employed and bath solutions were exchanged. The change of solutions was monitored by about 0.1% food dye (McCormick, Baltimore, MD) added to the bath solutions. Exchange of bath solutions took less than 30 s. The respective agents were applied to analyze whether ion channels were affected in opposite or synergistic ways by PKC or cGMP. Standard bath solution contained (in mM): NaCl 156, KCl 4, $CaCl_2$ 6, glucose 5, and *N*-2-hydroxyethylpiperazine-N′-2-ethanesulfonic acid (HEPES) 10. To block

voltage-dependent sodium channels 10^{-8} M tetrodotoxin (TTX) was added to all bath solutions. In order to determine Ca^{2+} dependence of ion channels, in few experiments, the bath solution contained a reduced Ca^{2+} concentration (10^{-7} M). In order to separate different cationic channels, the bath solutions contained 6 mM nickel, 1 or 10 mM zinc, 20 mM TEA, or 160 mM *N*-methyl-D-glucamin (NMDG). Bath solutions with reduced chloride concentration contained acetate-gluconate or D-gluconate salts (156 mM NaAc, 4 mM KAc, 6 mM $CaAc_2$, 10 mM HEPES, 5 mM glucose, and 10^{-8} M TTX).

The standard pipette solution contained (in mM): CsCl 160, $CaCl_2$ 0.5, 1,2-bis(o-aminophenoxy)ethane-N,N,N′,N′-tetraacetic acid (BAPTA) 1 (EGTA 11), and HEPES 10. The Ca^{2+} concentration was buffered to mimic low extracellular Ca^{2+} conditions, which were shown to stabilize otherwise transient Ca^{2+}-dependent and pheromone-dependent currents (Stengl 1993, 1994). Furthermore, 20 mM TEA, 10 mM zinc, or 6 mM Ca^{2+} were used in some experiments to isolate the interdependently activated ion channels. In analogy to bath solutions, pipette solutions with reduced chloride concentrations contained acetate-gluconate or D-gluconate salt.

The PKC activator phorbol ester (PMA; $n = 74$) was applied by puff application onto the recorded ORNs at a concentration of 10 nM (application volume <10 nl of the respective stock solution, for 2- to 10-ms pulse duration). In 2–10 ms pulses, the membrane-permeable cGMP analog 8bcGMP was applied at concentrations of 10 mM ($n = 49$), 100 μM ($n = 15$), 500 μM ($n = 15$), and 5 μM ($n = 5$) dissolved in extracellular solution. Furthermore, concentrations of 8bcGMP of 100 μM ($n = 2$) and 10 μM ($n = 7$) were pipetted into the bath solution. Because a detailed analysis of all application modes and concentrations did not reveal consistent differences, they were pooled. All control applications were puff applications with standard bath solution. Because of the typically delayed action of 8bcGMP, activation within 5 min after drug or control application was scored as application dependent.

Because different types of ion channels always opened at the same time and could not be obtained in isolation, 3 different channel classes were formed depending on their conductance. Small-conductance channels showed a maximal conductance of 20 ps at all potentials tested. Medium-conductance channels expressed conductances of more than 20 ps up to less than 100 ps. Also, rectifying cation channels with conductances of less than 20 ps at some potentials but larger than 20 ps at other potentials were grouped to the medium-conductance channels. Ion channels of more than 100-ps conductance were classified as large-conductance channels.

Electrophysiology

For patch clamp recordings, the culture medium was removed. Cell cultures were washed with about 1 ml of bath solution, and the dish was placed in the recording setup with about the same volume of bath solution. The culture dishes were continuously perfused with bath solution at a low flow rate, using a gravity feed perfusion system equipped with 6 reservoirs and a Teflon rotary valve (Rheodyne, Rohnert Park, CA). The cells were viewed with an inverted microscope (Axiovert 35 or 135, Zeiss, Göttingen, Germany) equipped with phase contrast optics and an additional heat filter (KG-1, Zeiss). ORNs were identified by their round or only slightly spindle-shaped soma of 5–10 μm diameter (Stengl and Hildebrand 1990). The patch clamp headstage and the drug application pipette were mounted on electronic micromanipulators (Luigs & Neumann, Ratingen, Germany) attached to aluminum profiles (X-95, Newport, Irvine, CA).

Inside-out patch clamp recordings were performed according to standard procedures (Hamill et al. 1981). For all recordings shown, upward deflections from the closed level are outward movements of positive ions and downward deflections from the closed level are inward movement of positive ions. Because the cultured cells deteriorated quickly in bath solutions with low Ca^{2+} concentration, the cell cultures were usually kept in standard bath solutions (high Ca^{2+}). Inside-out patches were excised into bath solutions containing high Ca^{2+} to search for Ca^{2+}-activated ion channels (Stengl 1993, 1994; Stengl et al. 1992, 1999). Inside-out configurations were verified at the beginning of the recording via application of voltage steps which should show fast transitions of currents, clear voltage control, and expected reversal potentials of previously characterized cation channels. Cell-attached recordings were not possible, because of electrode drift, which caused patch excision into the inside-out configuration.

Signals were amplified with an Axopatch 1D amplifier (Axon Instruments, Union City, CA), passed through the built-in antialiasing filter at a cutoff frequency of 2 kHz, digitized in a Digidata 1200B digitizer (Axon Instruments) at a sampling rate of 10 or 20 kHz, and stored and analyzed using pCLAMP software (versions 6 to 8, Axon Instruments). In addition, the signals were continuously recorded on a strip chart recorder (EasyGraf, Gould, Valley View, OH) and stored on DAT (DTR-1202, Bio-Logic, Claix, France). When signals were digitized offline from the tape, they were either passed through the amplifier or through an external antialiasing filter (900C/9L8L, Frequency Devices, Haverhill, MA) and digitized at different sampling rates, depending on the filter setting.

Data analysis of single-channel recordings

In single-channel recordings, single-unit currents were determined from amplitude histograms created with Fetchan 6 (pCLAMP). When the data had to be low-pass filtered to improve the signal-to-noise ratio, either the analog 8-pole Bessel filter of the amplifier was used to condition signals during off-line digitization from the DAT tape or the data were conditioned with the digital Gaussian filters

implemented in Fetchan 6 or Clampfit 8. The cutoff frequencies were typically between 200 Hz and 1 kHz, but in rare cases, cutoff frequencies as low as 50 Hz were also used. The amplitude histograms were fitted with Gaussian functions (second to sixth order) in pStat 6 with manual seeding of the initial values. The number of terms was determined manually, often by comparison of different models. Model comparison implemented in pStat was not used. Although the measures that describe the goodness of fit put out by the software were recorded, the quality of the fits was almost exclusively judged by eye. The current–voltage (I–V) relations were determined by 1 of 2 methods depending on the experiment. When a single or few copies of only one channel type were active for a longer period, the holding potential was stepped to different values and the single-unit currents were determined for each potential. Potentials are given as potential across the membrane. Because typically many copies of one channel type or different channels were open or exhibited transitions, voltage step protocols with step duration of 100 ms were applied. To exclude effects of voltage-dependent activation or inactivation, 2 types of step protocols were applied successively. First, the holding potential was stepped from negative (typically –120 mV) to positive (max 100 mV) potentials across the membrane in 20 mV increments. Then, the potential was stepped from 0 mV to increasing absolute potential values to negative and positive direction at alternating signs (0 mV, –20 mV, +20 mV, –40 mV, +40 mV, etc.). The I–V relations determined in this way were only used for further analysis if 1) the steady-state current before and after a step protocol was identical and 2) there was evidence for the contribution of single-unit currents to the steady-state current (such as transitions before or after the step protocols). In most cases, only outward currents at positive holding potentials allowed to discern single-channel openings for the calculation of I–V curves. Thus, single-channel conductances were usually calculated at positive command potentials. Generalized linear model analysis with binomial error distribution was used for statistical analysis to estimate channel activity in response to high intracellular Ca^{2+}, the PKC activator PMA, and/or 8bcGMP (Crawley 2002).

Results

To identify second messenger–dependent ion channels involved in sensitivity adjustment to odor concentration and duration, single-channel patch clamp recordings were performed on primary cell cultures of antennal ORNs of *M. sexta*. Ion channels were studied in response to high intracellular Ca^{2+}, the PKC activator PMA, and/or 8bcGMP. In inside-out patch clamp recordings in high Ca^{2+} bath solution, different ion channels were distinguished according to conductance, reversal potential, I–V relation, and pharmacology. We focused on the effects of PKC and 8bcGMP on nonselective cation channels of medium-sized conductance and characterized Ca^{2+}-dependent channels that are closed by PKC- and PKC-dependent ion channels that are closed by cGMP.

Ion channel classes observed after excision into high Ca^{2+} in the presence or absence of PMA and/or 8bcGMP

Because pheromone stimulation causes rises in intracellular Ca^{2+} and activates a sequence of Ca^{2+}-dependent cation channels (Stengl 1993, 1994; Stengl et al. 1999), we, therefore, excised inside-out patches into solutions with high Ca^{2+}. In a total of 116 patch clamp experiments, 3 classes of ion channels, small (≤20 ps), medium (between 20 and 100 ps), and large (>100 ps) were regularly recorded in high Ca^{2+} bath solution (Figures 1, 2, and 8). As judged from the reversal potential, from ion exchange-, and from blocking experiments, at least some of the small-conductance channels appeared to be Ca^{2+} channels (Figures 1 and 2; see Small-conductance (2-20 pS) ion channels). These channels were not further analyzed to focus on nonspecific cation channels. The medium-conductance channels were mostly nonselective cation channels because they reversed around 0 mV membrane potential under all ionic conditions and expressed considerable inward currents. Fewer K^+ channels with small outward currents at positive membrane potentials and without inward currents were also among the medium-conductance channels. The large-conductance channel-like events were apparently caused by Ca^{2+}-dependent, synchronized openings of chloride channels and nonselective cation channels as judged from the ion exchange and blocking experiments.

In the following, observations on patch excision-activated and PKC- and cGMP-dependent ion channels are summarized, normalized, quantified, and statistically analyzed (n = 213 experiments in 116 different recordings; Figure 1). Then, the most prominent types of nonselective cation channels, namely, about 30/35-ps, 40-ps, 55-ps, 60-ps, and 70-ps channels are further characterized. Recordings expressing very large currents without recognizable single-channel transitions were not included in the quantitative analysis.

Under control conditions (n = 57; Figure 1A), without application of 8bcGMP and in the absence of PMA, mostly small-conductance channels (10–20 ps) and some medium- (about 30 ps) and large-conductance (>100 ps) channels opened. Preexposure to PMA (n = 36; Figure 1B and 2) decreased the probability to detect 10-ps small- and >100-ps large-conductance channels. Instead, predominantly 40- and 60-ps medium-conductance channels opened, and few 70-ps medium-conductance channels were detected. Statistical analysis revealed a significant difference in the distribution of medium-conductance channels between control and the presence of PMA (Figure 1A,B; $P < 0.05$), with significantly more openings of 40-ps medium-conductance channels in the presence of PMA ($P < 0.05$).

In the presence of 8bcGMP (n = 78; Figure 1C, 6, and 7), 10-ps small-, 55- and 70-ps medium-, and >100-ps

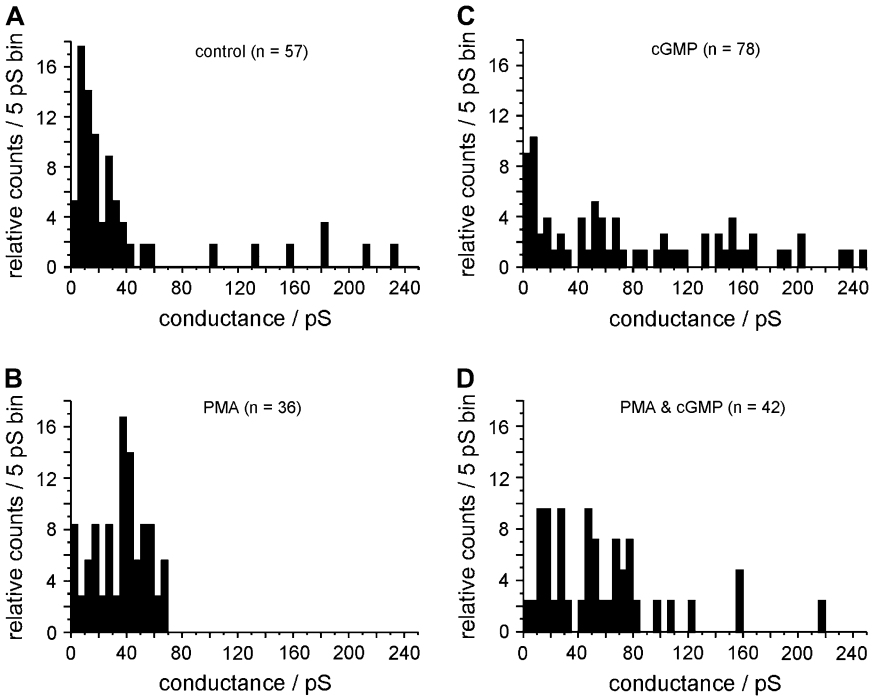

Figure 1 Frequency distribution histograms of single-channel conductances recorded with or without application of phorbol ester (PMA) and/or 8bcGMP at 40 to 60 mV holding potential. **(A)** In the absence of 8bcGMP and PMA, most recorded single-channels had a conductance below 60 ps. Single-channel conductances >100 ps were recorded occasionally. **(B)** After application of PMA, single-channels with 10 and >100 ps were less frequently recorded. Instead, single-channels with a conductance of about 40, 60, and 70 ps were recorded. **(C)** After application of 8bcGMP, there was a tendency to large single-unit conductances. Single-channel conductances of about 10, 55, 70, and >100 ps were recorded. The 40-ps conductances were absent. **(D)** After 8bcGMP and PMA application, fewer 10-ps small-conductance channels were distinguishable among the currents that developed. The 40-ps conductances were absent. For statistical analysis see text.

large-conductance channels were observed. The 30-ps medium-conductance channels were less frequently detected as compared with recordings in the absence of 8bcGMP (Figure 1A,B). Statistical analysis revealed a significant difference in the distribution of medium-conductance channels between the presence of PMA and 8bcGMP (Figure 1B,C; $P < 0.01$), with significantly more openings of 40-ps channels in the presence of PMA ($P < 0.01$). For the large-conductance channels, significant differences between control and the presence of 8bcGMP (Figure 1A,C; $P < 0.05$) as well as between the presence of PMA and 8bcGMP (Figure 1B,C; $P < 0.05$) were observed.

After 8bcGMP application and additional preexposure to PMA ($n = 42$, Figure 1D), small-conductance channels, and about 30- and 50-ps medium-conductance channels opened frequently. The 10-ps small- and 40 ps medium-conductance channels were less frequently recorded. Statistical analysis revealed a significant difference in the distribution of medium-conductance channels between the presence of 8bcGMP alone and the presence of 8bcGMP and PMA (Figure 1C,D; $P < 0.01$). The open probability of 10-ps small-conductance channels was significantly reduced in the presence of 8bcGMP and PMA as compared with the control (Figure 1A,D; $P < 0.05$).

In general, following application of PMA, the medium-conductance channels were observed more often and the detection of single-channel currents became very difficult. In most recordings, large currents (up to several tens of ns in aggregate conductance) developed some time after patch excision into high Ca^{2+} (58%), after PMA (31%), and also after 8bcGMP application (31%). Thus, no single-channel activity was distinguished. Only the fact that these large currents typically developed in the course of several 100 ms and occasionally inactivated later distinguished them from a broken seal. After patch excision into high Ca^{2+} and after PMA and/or 8bcGMP application, different ion channels activated together, before large currents developed. Therefore, it was not possible to completely characterize the different ion channels involved. In the following, ion channels recorded at least once in isolation are distinguished according to conductance, reversal potential, I–V relation, and pharmacology and are grouped into 3 classes, small-, medium-, and large-conductance ion channels.

Small-conductance (2–20 ps) ion channels

Small-conductance channels of 2- to 20-ps single-unit conductance were detected in some of the recordings ($n = 17$

out of 116). When the absence of other active channels allowed the analysis of their kinetics (n = 3), the small-conductance channels displayed dwell times of many seconds (Figure 2B). The fact that these channels were not recorded in the presence of Ca^{2+} channel blockers like 6 mM Ni^{2+} suggests that at least some of them are Ca^{2+} channels. Because they were obscured by larger channels in most recordings, a more detailed analysis was not possible.

Medium-conductance (20–100 ps) ion channels

Most ion channels with conductances between 20 and 100 ps were nonselective cation channels with a reversal potential around 0 mV and linear or rectified I–V relations. K^+-selective channels could be distinguished from nonselective cation channels by their small outward currents and the absence of inward currents. Without 20 mM TEA in the bath solution, nonselective cation channels were recorded in almost all experiments. Different subtypes of the medium-conductance channels were distinguished according to conductance, different I–V relations, pharmacology, and kinetics. The open times ranged from rapid flickering to dwell times of many seconds (Figures 3–7).

Under control conditions, the most frequently recorded subtype of medium-conductance channels had about 75 ps at negative potentials and about 35 ps at positive potentials and activated spontaneously after patch excision into bath solutions with high Ca^{2+} and Cs^+ pipette solution (Figure 3). In the presence of 20 mM TEA, these medium-conductance channels were blocked (n = 3). Once activated, these channels did not inactivate after switching to bath solution with reduced Ca^{2+} concentration (10^{-7} M; n = 11). This channel type belongs to the cation channels of about 30 ps in Figure 1.

Another type of medium-conductance channel of about 35 ps (Figure 4) was blocked by application of 8bcGMP. The inactivation of this channel was observed in isolation only once. In most experiments, this channel was obscured

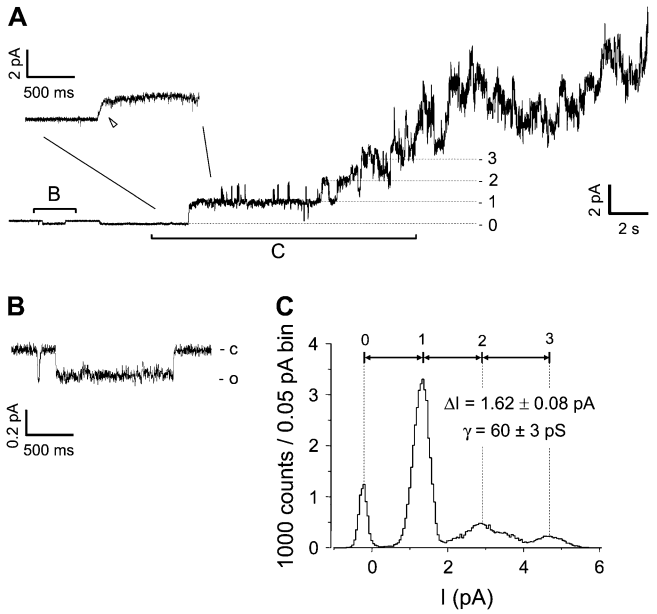

Figure 2 **(A–C)** Small- and medium-conductance channels in cultured moth ORNs. **(A)** A 60-ps channel was observed after previous PMA application in an inside-out recording at +27 mV membrane potential. PMA was present in the dish before patch excision. The enlarged insert shows slow channel opening due to nonresolved substates (arrowhead). **(B)** Before the activation of the medium-conductance channels a small-conductance channel with very long dwell times was active. This channel conducted inward currents at the positive membrane potential. **(C)** Amplitude histogram of the section indicated in A. The numbers above the peaks correspond to the current levels indicated in A. The differences in the current levels (ΔI) were 1.62 ± 0.08 pA, corresponding to a single-unit conductance (γ) of 60 ± 3 ps (mean ± standard deviation). After the activation of the third channel copy, distinct current levels could not be discerned anymore. Downward deflections from the closed state indicate inward current of positive ions from the patch electrode through the patch into the bath.

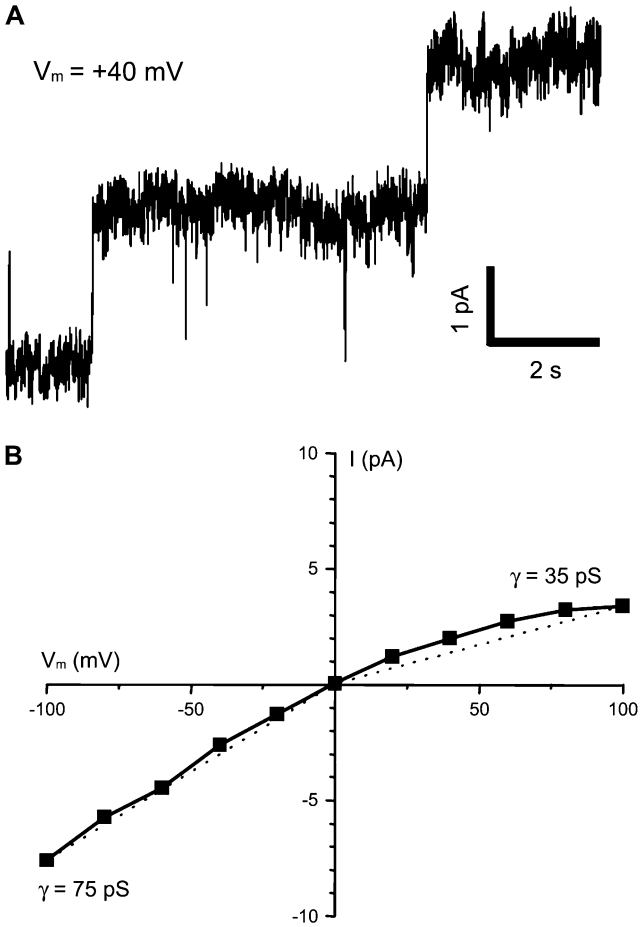

Figure 3 Patch excision activated a medium-conductance channel of about 35 ps at positive holding potentials. **(A)** A medium-conductance channel with dwell times of many seconds was active after patch excision. **(B)** A single-channel I–V relation showed that the medium-conductance channel is an inward rectifier with conductances (γ) of about 35 ps at positive potentials and 75 ps at negative potentials.

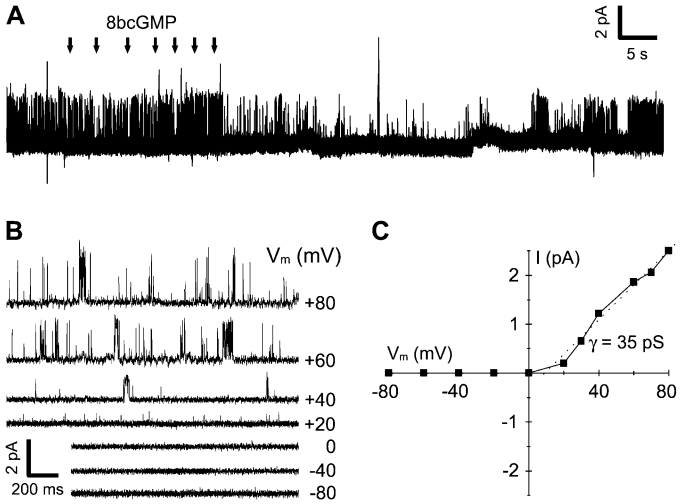

Figure 4 An outwardly rectifying medium-conductance channel of about 35 ps was transiently blocked by 8bcGMP. **(A)** The application of several pulses of 8bcGMP (10-mM stock solution, several nanoliters applied into 1 ml solution, arrows) to an inside-out patch at a membrane potential of +80 mV inhibited a single copy of an active channel. After about 40 s of wash, the channel gradually regained its original activity. **(B** and **C)** I–V relation of the same channel type obtained in a different inside-out recording. (B) The patch was kept at different potentials for several seconds, and the single-unit conductance was determined by amplitude histograms (data not shown). **(C)** While the channel conducted no Cs^+ inward currents, the slope conductance (γ) of the outward currents was about 35 ps.

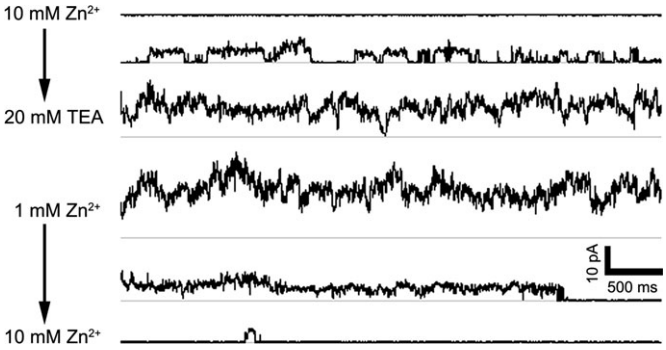

Figure 5 A medium-conductance channel of 40 ps was sensitive to 10 mM Zn^{2+} but was not blocked in the presence of 20 mM TEA. About 25 s after an inside-out patch held at V_m = +80 mV was exposed to 10 mM Zn^{2+} bath solution; all previously active channels were closed (upper trace). When zinc was washed out with 20 mM TEA, channel activity reappeared (second trace) until a large current developed without recognizable single-channel events (third trace). In a bath solution containing 1 mM Zn^{2+} (fourth trace), channel activity was not notably affected. Switching back to 10 mM Zn^{2+} blocked the channel activity again (bottom 2 traces). Note that distinct current levels were only determined during the wash out and wash in of 10 mM Zn^{2+} bath solution, as indicated by the arrows on the left. The amplitude histograms of traces 2 and 5 suggested a single-unit conductance of about 40 ps, with the presence of many substates (data not shown). The gray lines indicate the zero-current levels. Traces were separated by about 1 min each, except for the last 2 traces, which are consecutive.

by opening of other medium-conductance nonselective cation channels. Because this channel conducted no inward currents with Cs^+ in the patch pipette, it appears to be a potassium channel.

Application of PMA revealed medium-conductance channels of about 60 ps with reversal potentials around 0 mV and a linear conductance. Usually, this channel was recorded in ≥3 copies per patch (Figure 2A,C). Individual transitions between open and closed states took up to 100 ms, whereas sharp transitions occurred immediately before or after these slow transitions (n = 6 openings and 3 closings in different recordings). The individual transitions appeared to consist of several subconductance levels, which were too small to resolve. Spontaneous activation of the 60-ps channel always involved multiple copies in rapid succession, which suggests coupling among adjacent channels of the same type (Figure 2). The 60-ps channel was recorded more frequently after application of PMA (Figure 1) and was not detected in the presence of 20 mM TEA.

A subpopulation of medium-conductance channels activated spontaneously with a conductance of 40 ps at positive holding potentials. This channel was blocked by 10 mM but not by 1 mM Zn^{2+} in the bath solution (n = 2 out of 7 observations) and was not affected by 20 mM TEA (Figure 5). The 40-ps channel was more frequently observed in the presence of PMA (Figure 1). Activation of medium-conductance channels was also recorded with 10 mM Zn^{2+} in the pipette solution (n = 25 out of 31), indicating that only a subpopulation of medium-conductance channels is zinc sensitive.

After application of 8bcGMP, a 55-ps channel activated at +40 mV holding potential (Figure 6). This cGMP-dependent ion channel showed a reversal potential around 0 mV and reduced inward current in the presence of 10 mM Zn^{2+} in the pipette solution (Figure 7). The 55-ps channel was rarely seen during control conditions (Figure 1A) but was recorded more frequently after 8bcGMP application (Figures 1C,D, 6, and 7). It is a nonselective cation channel which appears to be blocked by divalent cations (Figure 7).

A 70-ps channel was blocked by application of 20 mM TEA (data not shown). This medium-conductance channel was only observed in the presence of 8bcGMP with or without PMA (Figure 1). It activated and inactivated slowly at –40 mV holding potential and expressed larger outward and reduced inward currents with Cs^+ in the pipette solution. Thus, the 70-ps channel appears to be a potassium channel.

Large-conductance ion channels (>100 ps)

In addition to the small- and the medium-conductance channels, large-conductance channels of >100 ps single-unit conductance were recorded. Like most of the medium-conductance channels, they typically activated after patch excision without drug application or other obvious changes in the conditions. Frequently, the activation was correlated with the activation of medium-conductance channels, which suggests an unknown coupling mechanism. Apparent

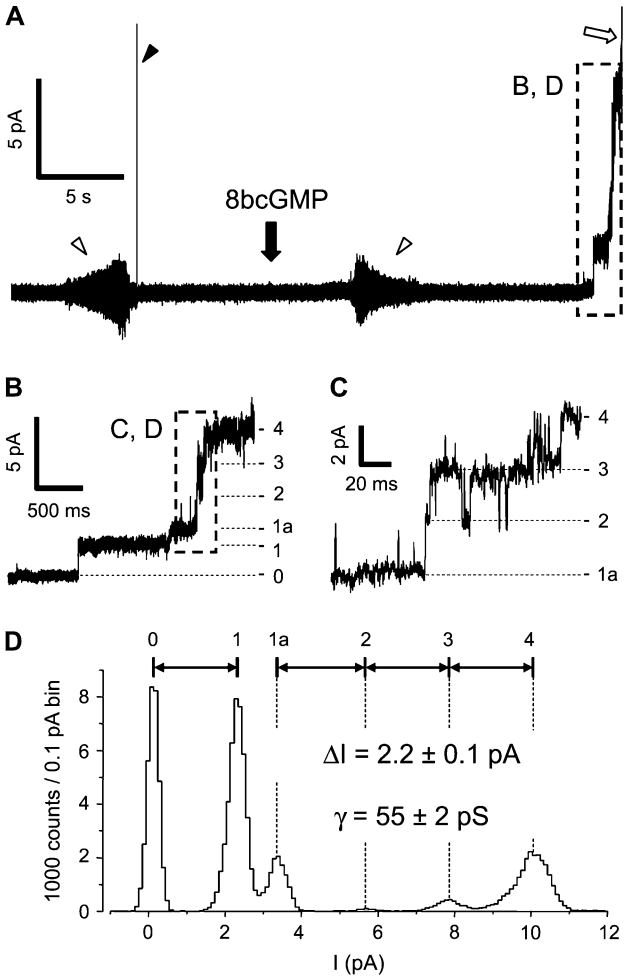

Figure 6 A 55-ps channel opened after application of 8bcGMP. **(A)** At least 4 copies of a medium-conductance channel activated in an inside-out patch after puff application of 8bcGMP (10 mM stock solution) at +40 mV holding potential. The high-frequency artifacts (open arrowheads) occurred when the application pipette was moved into and out of the bath. The large capacitive transient (filled arrowhead) occurred when the application pipette first touched the surface of the bath. About 20 s after drug application to the vicinity of the cell, several copies of a channel activated in rapid succession (indicated section shown at an enlarged time scale in **B**). About 2 s after the first observed channel activity, a current of >100 pA developed (open arrow; truncated), in which no single-channel currents were resolved. **(C)** Enlarged view of the section indicated in B shows single-channel events. **(D)** Amplitude histogram of the section shown in B. The differences in the current levels (ΔI) were 2.2 ± 0.1 pA, corresponding to a single-unit conductance (γ) of 55 ± 2 ps (mean ± standard deviation). Another channel type with a smaller conductance caused the transition from current level 1 to 1a. Current levels in B–D correspond to each other.

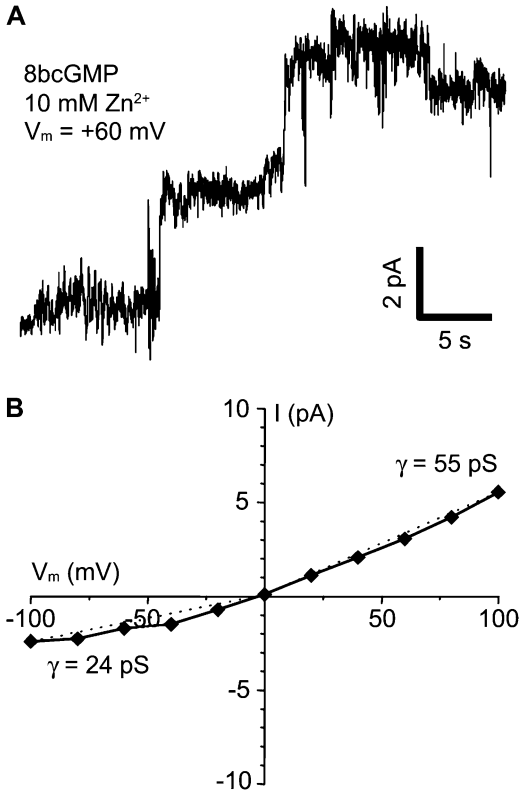

Figure 7 Patch excision activated a medium-conductance channel of about 55 ps at positive holding potentials. **(A)** Two copies of a 55-ps medium-conductance channel activated after 8bcGMP application. **(B)** A single-channel I–V relation obtained with voltage step protocols suggested a linear, zero-crossing current of 55-ps conductance (γ) at positive potentials. The inward currents were probably reduced by 10 mM Zn^{2+} included in the pipette solution.

single-unit conductances of up to 550 ps were detected (Figures 1 and 8), in one recording even 1.7 ns. The transitions between the conductance states suggested the presence of multiple substates or of multiple coupled ion channels. In most observations, the apparent single-unit conductance was below 250 ps (Figure 8). Once activated, the large-conductance channels were affected only partly by replacing all cations in the bath solution with NMDG (n = 5 out of 7), a very large cation impermeant to most cation channels. The tested agents known as chloride channel blockers (6 mM Ni^{2+}, 10 mM Zn^{2+}, 1 mM 4-acetamido-4′-isothiocyanostilbene-2, 2′ disulphonic acid, 1 mM 4,4′-diisothiocyanostilbene-2,2′-disulfonic acid, 1 mM niflumic acid, 500 µM anthracene-9-carboxylic acid, and 100 µM picrotoxin) did not influence the medium-conductance channels and only partly affected the large-conductance channels (n > 10). Thus, the large-conductance channels were apparently conducted by nonselective cation and chloride channels, directly or indirectly activated by Ca^{2+}.

Discussion

In primary cell cultures of ORNs of *M. sexta*, we analyzed ion channels modulated by PKC and cGMP with inside-out patch clamp recordings. The large diversity of interdependently activated ion channels allowed no detailed analysis but only a very general characterization of individual channels and their pharmacology in single-channel recordings. Nevertheless, new PKC- and cGMP-dependent ion channels were identified, and interactions between the second

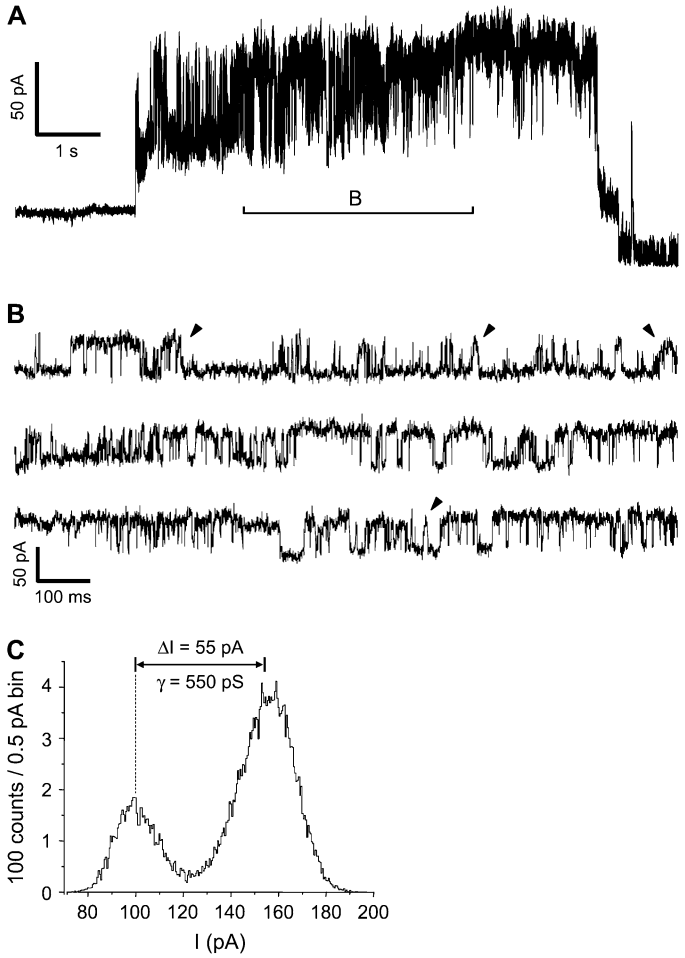

Figure 8 The large-conductance channels (>100 ps) were not blocked by TEA and Zn^{2+}. Inside-out recording at a membrane potential of +100 mV exposed to 20 mM TEA in the bath and 10 mM Zn^{2+} in the pipette solution. **(A)** From the open state of a different channel type, a large-conductance channel activated spontaneously. After about 7.5 s the large-conductance channel and the initially open channels inactivated, revealing several substates. **(B)** The section indicated in A at an enlarged timescale. Individual transitions suggest a number of substates (arrowheads), which cannot be resolved in an amplitude histogram **(C)**.

messenger systems were detected, hinting at novel mechanisms of sensitivity modulation in the insect olfactory system.

Second messenger–mediated ion channels

Because ORNs can be clearly distinguished from other cell types in primary cell cultures (Stengl and Hildebrand 1990), the recorded ion channels probably belong to the olfactory signal transduction cascades. It is not possible, however, to distinguish between pheromone- and general odor-responsive ORNs from morphological markers only. Furthermore, it is not possible to determine whether different ORN classes exist, which express different sets of ion channels. The fact that in previous studies Ca^{2+}-dependent and PKC-dependent currents were expressed in almost all recordings suggests that the respective ion channels are common to most ORNs and are shared between pheromone- and general odor-transduction cascades (Stengl et al. 1992; Stengl 1993, 1994). Whether all ORNs or only subgroups also possess cGMP-dependent ion channels remains to be examined.

At least some of the small-conductance channels recorded after patch excision into high Ca^{2+} are likely to be voltage-dependent Ca^{2+} channels because they were never observed in the presence of Ca^{2+} blockers (Stengl 1994; Lucas and Shimahara 2002). Future whole-cell studies will examine Ca^{2+} channels in ORNs of *M. sexta* in more detail because a thorough single-channel analysis was not possible.

The 30–35 ps inwardly rectified cation channel (Figures 1A and 3) resembles the pheromone-activated cation channel, which was reported by Stengl et al. (1992) with a conductance of 20 ps at +25 mV and 50 ps at –100 mV holding potential. Different patch clamp configurations and ionic solutions may account for the differences in the conductance of this channel. In addition, this channel appears to be identical to the 37 ps (at +30 mV) cation channel which activated spontaneously after excision into the outside-out mode (Stengl et al. 1992; Stengl 1993). The 30- to 35-ps channel is a Ca^{2+}-dependent cation channel and apparently underlies the second pheromone-dependent inward current component. It opened in Ca^{2+} concentrations higher than 10^{-6} M and was blocked by a Ca^{2+}-dependent negative feedback. The fact that the 30- to 35-ps channel opened readily over the course of minutes in excised patches suggests that the high Ca^{2+} concentrations could not exert any negative feedback because cytosolic factors, such as calmodulin, were missing. The channel was not affected by PKC activation but was less often observed in the presence of cGMP. In ORNs of the silkmoth *Antheraea polyphemus*, a Ca^{2+}-activated cation channel of about 48-ps conductance was blocked by cGMP (Zufall and Keil 1991). Because statistical analysis of this channel type was not possible, it could not be conclusively shown that this cation channel type in *M. sexta* is also blocked by cGMP.

The other type of 35-ps channel, which was blocked by cGMP, is most likely the previously described 30-ps delayed rectifier potassium channel, which was also blocked by cGMP as well as cyclic adenosine monophosphate (cAMP) and adenosine triphosphate (ATP) (Zufall et al. 1991). This rapidly activating channel opens immediately after pheromone application, even before the cell depolarized (Stengl et al. 1992). If this channel type is present in the axons of ORNs, it contributes to the repolarization after the Na^{+} channel opening and, thus, determines the duration of interspike intervals (Dolzer et al. 2001). It will be interesting to determine whether the 35-ps channel belongs to the KCNQ ion channel family, underlying the M current in other species (reviewed by Hille 2001).

Among the PKC-dependent activated channels, only the 40-ps channel was significantly more often observed in the

presence of PMA. Because the 40-ps channel was not affected by TEA, it can only partly underlie the previously described PKC-dependent non-Ca^{2+}-permeable, mostly TEA-blockable cation current which occurred after long pheromone stimulation (Stengl 1993, 1994). So far, the 60-ps PKC-dependent cation channel is the best candidate for the TEA-blockable, pheromone-dependent inward current component and further experiments need to test this hypothesis. The 40-ps cation channel which was not affected by TEA has not been described before. Also, the 70-ps channel which was only observed in the presence of 8bcGMP and PMA awaits a further characterization. Because it was blocked by TEA and showed small, slowly activating outward and no inward currents, it seems to be a delayed rectifier potassium channel with slow kinetics. Whether this channel is encoded by the ether a-go-go (eag) potassium channel gene cloned from *M. sexta* (Keyser et al. 2003) remains to be examined.

The 55-ps cGMP-dependent activated cation channel shared properties with other CNG channels described from vertebrates (Kaupp and Seifert 2002; Craven and Zagotta 2006; Pifferi et al. 2006). It appeared to be a nonselective cation channel, which was blocked via Zn^{2+} in the recording electrode. However, in contrast to vertebrate CNG channels, it was not affected by the high intracellular Ca^{2+} concentration. It remains to be tested whether addition of calmodulin together with high Ca^{2+} would block the 55-ps channel. Cloning and expression of CNG channels from *M. sexta* will facilitate the characterization of this cation channel in the future. Surprisingly, no dose dependency was detected with the different cGMP concentrations tested. Apparently, all cGMP-dependent channels opened in concerted action. Whether this was due to a Ca^{2+}-dependent coupling mechanism remains to be examined.

The >100-ps large-conductance channels expressed very large currents which appeared to conduct nonselectively cations and anions and apparently synchronized their channel openings via Ca^{2+}-dependent mechanisms. Because no reliable blockers of chloride channels in *M. sexta* are available, the further characterization of these channels is difficult and requires cloning and expression studies.

A hypothesis of sensitivity modulation in ORNs

In moth ORNs, pheromone stimuli open a characteristic sequence of 3 Ca^{2+}-dependent inward currents. The first 2 channels are downregulated by Ca^{2+}-dependent negative feedback, whereas the third, a PKC-dependent inward current, is stable in the presence of second-long pheromone stimulation (Stengl et al. 1992; Stengl 1993, 1994). Furthermore, minute-long pheromone stimulation elevates cGMP levels in ORNs of *M. sexta* (Stengl et al. 2001). Thus, cGMP elevations in ORNs correlate with the time course of long-term adaptation, whereas the PKC-dependent currents rather correlate with the time course of short-term adaptation and Ca^{2+}/calmodulin-dependent negative feedback with mechanisms of desensitization. We, therefore, suggest that different sets of depolarizing and hyperpolarizing ion channels, controlled by intracellular Ca^{2+}, Ca^{2+}-dependent kinase activity, and cyclic nucleotide concentrations, are responsible for the sliding modulation of pheromone sensitivity during short- and long-term adaptation. Our findings are consistent with this hypothesis because different sets of ion channels were observed in the presence or absence of high intracellular Ca^{2+}, 8bcGMP, or PKC activators. Further, whole-cell and perforated patch clamp recordings will investigate whether the ORNs of *M. sexta* express ion channels that are activated differentially by Ca^{2+}, 8bcGMP, or PKC activators. Finally, cloning and expression of the different second messenger–mediated ion channels together with RNA_i will further test our hypothesis.

Funding

Deutsche Forschungsgemeinschaft grants STE 531/5-1, 10-1, 10-2, and 10-3 to M.S.

Acknowledgements

The authors would like to thank Thomas Hörbrand, Karin Fischer, Holger Schmidt, Markus Hammer, Marion Zobel, Patrick Winterhagen, and Klaus Isselbächer for insect rearing, Ingrid Jakob and Philippe Lucas for valuable discussions, and Günther Stöckl for technical help. This manuscript was significantly improved with the help of Dr Uwe Homberg, Dr A Steinbrecht, and unknown referees.

References

Boekhoff I, Seifert E, Göggerle S, Lindemann M, Krüger BW, Breer H. 1993. Pheromone-induced second-messenger signaling in insect antennae. Insect Biochem Mol Biol. 23(7):757–762.

Boekhoff I, Strotmann J, Raming K, Tareilus E, Breer H. 1990. Odorant-sensitive phospholipase C in insect antennae. Cell Signal. 2:49–56.

Craven KB, Zagotta WN. 2006. CNG and HCN channels: two peas, one pod. Annu Rev Physiol. 68:375–401.

Crawley MJ. 2002. Statistical computing: an introduction to data analysis using S-Plus. New York: John Wiley & Sons.

Dolzer J, Fischer K, Stengl M. 2003. Adaptation in pheromone-sensitive trichoid sensilla of the hawkmoth *Manduca sexta*. J Exp Biol. 206: 1575–1588.

Dolzer J, Krannich S, Fischer K, Stengl M. 2001. Oscillations of the transepithelial potential of moth olfactory sensilla are influenced by octopamine and serotonin. J Exp Biol. 204:2781–2794.

Flecke C, Dolzer J, Krannich S, Stengl M. 2006. Perfusion with cGMP analogue adapts the action potential response of pheromone-sensitive sensilla trichoidea of the hawkmoth *Manduca sexta* in a daytime-dependent manner. J Exp Biol. 209:3898–3912.

Hamill OP, Marty A, Neher E, Sakmann B, Sigworth FJ. 1981. Improved patch-clamp techniques for high-resolution current recording from cells and cell-free membrane patches. Pflügers Arch. 391:85–100.

Hille B. 2001. Ion channels of exitable membranes. 3rd ed. Sunderland (MA): Sinauer Associates.

Jindra M, Huang JY, Malone F, Asahina M, Riddiford LM. 1997. Identification and mRNA developmental profiles of two ultraspiracle isoforms in the epidermis and wings of *Manduca sexta*. Insect Mol Biol. 6:41–43.

Kaissling K-E, Zack-Strausfeld C, Rumbo ER. 1986. Adaptation processes in insect olfactory receptors: their relation to transduction and orientation. Chem Senses. 11:574–577.

Kaupp UB, Seifert R. 2002. Cyclic nucleotide-gated ion channels. Physiol Rev. 82:769–824.

Keyser MR, Anson BD, Titus SA, Ganetzky B, Witten JL. 2003. Molecular characterization, functional expression, and developmental profile of an ether a-go-go K^+ channel in the tobacco hornworm *Manduca sexta*. J Neurobiol. 55:73–85.

Lucas P, Shimahara T. 2002. Voltage- and calcium-activated currents in cultured olfactory receptor neurons of male *Mamestra brassicae* (Lepidoptera). Chem Senses. 27:599–610.

Marion-Poll F, Tobin TR. 1992. Temporal coding of pheromone pulses and trains in *Manduca sexta*. J Comp Physiol [A]. 171:505–512.

Matthews HR, Reisert J. 2003. Calcium, the two-faced messenger of olfactory transduction and adaptation. Curr Opin Neurobiol. 13:469–475.

Pifferi S, Boccaccio A, Menini A. 2006. Cyclic nucleotide-gated ion channels in sensory transduction. FEBS Lett. 580:2853–2859.

Redkozubov A. 2000. Guanosine 3′,5′-cyclic monophosphate reduces the response of the Moth's olfactory receptor neuron to pheromone. Chem Sens. 25:381–385.

Stengl M. 1993. Intracellular-messenger-mediated cation channels in cultured olfactory receptor neurons. J Exp Biol. 178:125–147.

Stengl M. 1994. Inositol-trisphosphate-dependent calcium currents precede cation currents in insect olfactory receptor neurons *in vitro*. J Comp Physiol [A]. 174:187–194.

Stengl M, Hildebrand JG. 1990. Insect olfactory neurons *in vitro*: morphological and immunocytochemical characterization of male-specific antennal receptor cells from developing antennae of male *Manduca sexta*. J Neurosci. 10(3):837–847.

Stengl M, Ziegelberger G, Boekhoff I, Krieger J. 1999. Perireceptor events and transduction mechanisms in insect olfaction. In: Hansson BS, editor. Insect olfaction. Berlin: Springer. p. 49–66.

Stengl M, Zintl R, de Vente J, Nighorn A. 2001. Localization of cGMP immunoreactivity and of soluble guanylyl cyclase in antennal sensilla of the hawkmoth *Manduca sexta*. Cell Tissue Res. 304: 409–421.

Stengl M, Zufall F, Hatt H, Hildebrand JG. 1992. Olfactory receptor neurons from antennae of developing male *Manduca sexta* respond to components of the species-specific sex pheromone in vitro. J Neurosci. 12: 2523–2531.

Wegener JW, Breer H, Hanke W. 1997. Second messenger-controlled membrane conductance in locust (*Locusta migratoria*) olfactory neurons. J Insect Physiol. 43:595–603.

Zack-Strausfeld C, Kaissling K-E. 1986. Localized adaptation processes in olfactory sensilla of Saturniid moths. Chem Senses. 11:499–512.

Ziegelberger G, van den Berg MJ, Kaissling K-E, Klumpp S, Schultz JE. 1990. Cyclic GMP levels and guanylate cyclase activity in pheromone-sensitive antennae of the silkmoths *Antheraea polyphemus* and *Bombyx mori*. J Neurosci. 10(4):1217–1225.

Zufall F, Keil TA. 1991. A calcium-activated nonspecific cation channel from olfactory receptor neurons of the silkmoth *Antheraea polyphemus*. J Exp Biol. 161:455–468.

Zufall F, Leinders-Zufall T. 2000. The cellular and molecular basis of odor adaptation. Chem Senses. 25:473–481.

Zufall F, Stengl M, Franke C, Hildebrand JG, Hatt H. 1991. Ionic currents of cultured olfactory receptor neurons from antennae of male *Manduca sexta*. J Neurosci. 11(4):956–965.

Accepted June 19, 2008